Available online at www.sciencedirect.com

ScienceDirect

www.elsevier.com/locate/jes

JES JOURNAL OF ENVIRONMENTAL SCIENCES

www.jesc.ac.cn

Sorption kinetics of parent and substituted PAHs for low-density polyethylene (LDPE): Determining their partition coefficients between LDPE and water (K_{LDPE}) for passive sampling

Pei Lei[1,2,3], *Jinjie Zhu*[1], *Ke Pan*[3], *Hong Zhang*[2,4,*]

1. *State Key Laboratory of Pollution Control and Resources Reuse, School of the Environment, Nanjing University, Nanjing 210023, China*
2. *State Key Laboratory of Environmental Aquatic Chemistry, Research Center for Eco-Environmental Sciences, Chinese Academy of Sciences, Beijing 100085, China*
3. *Institute for Advanced Study, Shenzhen University, Shenzhen 518060, China*
4. *University of Chinese Academy of Sciences, Beijing 100049, China*

ARTICLE INFO

Article history:
Received 5 May 2019
Revised 31 July 2019
Accepted 31 July 2019
Available online 6 August 2019

Keywords:
Low-density polyethylene (LDPE)
PAHs
Substituted PAHs (SPAHs)
Freely dissolved concentrations
Passive sampling

ABSTRACT

Low-density polyethylene (LDPE) has been widely used as a sorbent for passive sampling of hydrophobic organic contaminants (HOCs) in aquatic environments. However, it has seen only limited application in passive sampling for measurement of freely dissolved concentrations of parent and substituted PAHs (SPAHs), which are known to be toxic, mutagenic and carcinogenic. Here, the 16 priority PAHs and some typical PAHs were selected as target compounds and were simultaneously determined by gas chromatography–mass spectrometer (GC–MS). Some batch experiments were conducted in the laboratory to explore the adsorption kinetics of the target compounds in LDPE membranes. The results showed that both PAHs and SPAHs could reach equilibrium status within 19–38 days in sorption kinetic experiments. The coefficients of partitioning between LDPE film (50 μm thickness) and water (K_{LDPE}) for the 16 priority PAHs were in good agreement with previously reported values, and the values of K_{LDPE} for the 9 SPAHs are reported in this study for the first time. Significant linear relationships were observed, i.e., $\log K_{LDPE} = 0.705 \times \log K_{OW} + 1.534$ for PAHs ($R^2 = 0.8361$, $p < 0.001$) and $\log K_{LDPE} = 0.458 \times \log K_{OW} + 3.092$ for SPAHs ($R^2 = 0.5609$, $p = 0.0077$). The selected LDPE film was also proven to meet the condition of "zero sink" for the selected target compounds. These results could provide basic support for the configuration and *in situ* application of passive samplers.

Introduction

The freely dissolved concentrations of hydrophobic organic contaminants (HOCs) are generally known to be indicative of what is bioavailable for benthic organisms, and as well as for potential human exposure through aquatic food webs (Chen et al., 2008; Gilbert et al., 2015; Lin et al., 2018a). However, their freely dissolved concentrations are difficult to determine and

* *Corresponding author. E-mail:* hongzhang@rcees.ac.cn (Hong Zhang).

https://doi.org/10.1016/j.jes.2019.07.021

might be overestimated by some conventional methods, e.g., centrifugation or filtration, due to the high affinity between dissolved organic matter (DOM) or colloids and HOCs in waters (Cornelissen et al., 2008; Li et al., 2018; Moeckel et al., 2014). Over the past decades, effective alternatives (e.g., passive sampling) have been developed to overcome some of these difficulties (Booij et al., 2016; Lydy et al., 2014). Passive samplers, such as semipermeable membrane devices (Mutzner et al., 2019), silicone rubbers (Ahrens et al., 2018), polyoxymethylene (Arp et al., 2015) and polyethylene devices (Lao et al., 2019), have been applied for measurement of freely dissolved concentrations of a wide range of HOCs (Lei et al., 2018b; Mayer et al., 2014).

In particular, passive samplers using low-density polyethylene (LDPE) as the sorbent phase have been widely used to measure freely dissolved HOCs (Borrelli et al., 2018; Sacks and Rainer, 2011; Valderrama et al., 2016). LDPE membrane is made of a micro-porous polymer, which can allow dissolved molecular species to freely pass through the membrane while the colloids or macromolecular organic matter are kept outside (Booij et al., 1998; Tcaciuc et al., 2015). Because they are biomimetic, cost-effective and technically simple (Joyce et al., 2016; Lao et al., 2019; Lohmann et al., 2017), LDPE passive samplers yield freely dissolved concentrations of HOCs without physical protection in aquatic environments (Liu et al., 2017). Therefore, it is critical to obtain the partition coefficients for HOCs between the absorbed phase of the passive sampler and the aqueous phase in the laboratory before exploring their freely dissolved concentrations, bioavailability and toxicity in field applications (Bao et al., 2012; Zhu et al., 2018).

Among the most ubiquitous environmental HOCs of high global concern, polycyclic aromatic hydrocarbons (PAHs) have been widely detected in aquatic systems such as lakes, rivers and wetlands (Lei et al., 2018a; Meng et al., 2019; Thuy et al., 2018). Due to their potential carcinogenicity, teratogenicity and mutagenicity, 16 PAHs have been regulated as priority pollutants by the USEPA. Notably, some substituted PAHs (SPAHs), e.g., nitro-PAHs (NPAHs), methyl-PAHs (MPAHs) and oxy-PAHs (OPAHs), can be produced from their parent PAHs via chemical or microbiological processes (Kojima et al., 2010; Qiao et al., 2016). Like their parent PAHs, they can also be directly introduced into aquatic systems by anthropogenic activities, such as those from municipal wastewater in urban areas, incomplete combustion and spillage of fossil fuel, and vehicle exhaust (Gómez et al., 2012; Manolis and Stephanou, 2007; Qiao et al., 2014a). Since they are more toxic and bioaccumulative than their corresponding parent PAHs (Knecht et al., 2011; Wang et al., 2011), SPAHs have drawn much attention in recent years. Due to technical analysis limitations, SPAHs in aquatic systems have been relatively less studied than their parent PAHs. Thus, the freely dissolved concentrations of SPAHs by passive sampling has seldom been reported (Hawthorne et al., 2011).

To address this issue, 16 parent PAHs and some typical SPAHs were synchronously analyzed by gas chromatography–mass spectrometer (GC–MS) in this study. The kinetic adsorption processes of these targets were explored and their LDPE-water partition coefficients (K_{LDPE}) were determined by laboratory calibration. The sorbent, i.e., LDPE, was also tested to verify whether it could meet the "zero sink" assumption in this study, to provide fundamental data support for subsequent passive sampler design and *in situ* application.

1. Materials and methods

1.1. Chemicals, experimental materials, and preparation

Sixteen priority parent PAHs and thirteen typical SPAHs were selected as target compounds in this study, and their physical and chemical properties are shown in Appendix A Table S1 and S2. Sixteen parent PAHs, including Naphthalene (Nap), Acenaphthylene (Acy), Acenaphthene (Ace), Fluorene (Fluo), Phenanthrene (Phe), Anthracene (Ant), Fluoranthene (Flua), Pyrene (Pyr), Benzo[*a*]anthracene (BaA), Chrysene (Chry), Benzo[*b*]-fluoranthene (BbF), Benzo[k]fluoranthene (BkF), Benzo-[a]pyrene (BaP), Indeno[1,2,3-*c*,*d*]pyrene (IncdP), Dibenz[a,h]-anthracene (DBA) and Benzo[*g*,*h*,*i*]perylene (BghiP), in a 1 mL mixed standard solution (200 mg/L), were purchased from AccuStandard Inc., New Haven, USA. Thirteen individual SPAH reference materials, including (1) five NPAHs: 2-Nitrofluorene (2-NF, 100 mg in 100% solid), 9-Nitroanthrancene (9-NA, 100 μg/mL in toluene), 3-Nitrofluoranthene (3-NF, 100 μg/mL in toluene), 1-Nitropyrene (1-NP, 10 mg in 99.8% solid), and 7-nitrobenz[*a*]anthracene (7-NBA, 100 μg/mL in toluene); (2) four MPAHs: 3,6-Dimethylphenanthrene (3,6-DMP, 10 mg in 100% solid), 2,6-Dimethylphenanthrene (2,6-DMN, 10 mg in 100% solid), 2-Methylnaphthalene (2-MN, 10 mg in 100% solid), and 1-Methylfluoranthene (1-MF, 10 μg/mL in acetonitrile); (3) four OPAHs: 9-Fluorenone (9-FL, 50 mg in 100% solid), Anthraquinone (AQ, 10 μg/mL in acetonitrile), 2-Methyl-9,10-anthranquinone (2-MAQ, 10 mg in 100% solid), and benz[*a*] anthracene-7,12-dione (BA-7,12-D, 50 μg/mL in toluene) were also obtained from AccuStandard Inc., New Haven, USA.

Five deuterated PAHs in toluene (4 mg/mL), i.e., naphthalene-d8 (Nap-d8), acenaphthene-d10 (Ace-d10), phenanthrene-d10 (Phe-d10), chrysene-d12 (Chry-d12) and perylene-d12 (Pery-d12), were also obtained from AccuStandard Inc., New Haven, USA, to indicate the recovery rates for the whole process. Internal standards, i.e., 2-Fluorobiphenyl (2-FB, 2.0 mg/mL dissolved in dichloromethane) and 2,2′,3,3′, 4,4′,5,5′,6,6′-Decachlorobiphenyl (PCB209, 100 μg/mL in isooctane) were purchased from Aldrich Chemical Co, Inc., Gillingham, Dorset, UK for quantitative analysis of the targets. Organic solvents of HPLC grade (4 L), e.g., dichloromethane (DCM), *n*-hexane (HEX), methanol (MeOH) and acetone (ACE), were purchased from J. T. Baker, USA. Anhydrous sodium sulfate was baked at 450°C for 4 hr before use, then cooled down to room temperature and transferred to a vacuum desiccator. Some tools, e.g., copper wire, tweezers, scissors and glass rods, were immersed in HEX in a cleaning process using 20 kHz ultrasound before use. Laboratory glassware was cleaned with a chromic acid mixture for 4 hr, then washed with tap water, followed by washing with purified water three times, and finally oven-dried at 450°C for 4 hr before use.

The LDPE film (50 μm thickness) was purchased from TRM manufacturing, Corona, CA, USA. The commercial sheets were cut into identical strips, i.e., 1 cm × 2 cm, about 8 mg in weight. These strips were extracted in sequence with DCM, MeOH and ultrapure water for 48, 24, and 24 hr respectively. Then, they were immersed in ultrapure water until use to avoid contamination in the air (Bao et al., 2012). Prior to use, these pre-cleaned strips were placed in a high frequency ultrasound bath (10 min, 40 kHz and a power of 80 W) to remove bubbles on their surface. Meanwhile, another kind of LDPE film (50 μm thickness), purchased from Runfang Co. Ltd., Zhenjiang, China, was subjected to the same pretreatments for comparison purposes to determine K_{LDPE} values in this study (described in Section 2.3).

1.2. Sorption kinetic experiments

The sorption kinetic experiments were carried out by measuring the concentrations of the targets in LDPE and water phase at different time points. Each glass media bottle (FB800-1000, Fisher) with 1 L ultrapure water was spiked with the target compounds at an initial concentration of 0.05 μg/L. This concentration was comparable to their environmental concentrations in rivers or lakes. For example, MPAHs, OPAHs and PAHs were found to be at levels of 0.02–0.40, 0.06–0.19 and 0.16–1.20 μg/L in water samples from the Haihe River System, North China (Qiao et al., 2014b), and 16 priority PAHs concentrations in the surface pore water from the northern bays of Taihu Lake were in the range of 1.58–3.03 μg/L (Lei et al., 2016). Sodium azide (NaN_3) was added into each bottle at 200 mg/L to inhibit microbial activity. The mixture was stirred at 100 r/min for 2 hr to evenly mix the solution. Then, three duplicate strips of LDPE, penetrated with clean copper wire to prevent their sticking together, were placed into each container. All these bottles were covered with their caps, sealed with Parafilm, and then kept in a shaking incubator at 20 ± 1°C with 100 r/min. The losses of the targets due to adsorption onto the glass container could be neglected (Bao et al., 2011; Yang et al., 2007a). The sampling time points were set at day 3, 8, 15, 25, 40 and 80.

At each time point, the LDPE strips were taken out and immediately rinsed with ultrapure water. Then, these strips were successively extracted with 10 mL DCM for 24 hr and 10 mL HEX for 24 hr. When measuring target compounds in liquid samples, the remaining water was concentrated by solid phase extraction (SPE) with Sep-Pak C18 cartridges (6 mL, 500 mg, Supelco). The details of this procedure were described in detail elsewhere (Qiao et al., 2013). Briefly, the cartridges were pre-conditioned by 5 mL each of dichloromethane, methanol and ultrapure water in sequence. After loading of the liquid samples, the cartridges were eluted by 10 mL DCM and 5 mL HEX sequentially. The extract was condensed and solvent-exchanged to HEX, and again concentrated to less than 1 mL. Anhydrous sodium sulfate was used to remove residual water. The extract was finally concentrated to 200 μL under a gentle nitrogen stream. The internal standards were added to each sample before instrumental analysis.

1.3. Simultaneous detection of the selected substituted and parent PAHs

Rather than a 5MS column, it has been reported that GC–MS equipped with a 17MS column performed better at separating and detecting parent PAHs and SPAHs due to its suitable polarity (Forsberg et al., 2011; Qiao et al., 2013). Therefore, a GC–MS (Perkin Elmer Clarus SQ 8) equipped with an Elite-17MS column was used in this study. This column is a cross band of 50% phenyl-50% methyl polysiloxane, with dimensions of 30 m × 0.25 mm × 0.25 μm (Cat# N9316538, Serial 1265365).

The GC temperature program from a previous report was adopted with minor revision (Qiao et al., 2013): held initially at 60°C for 1 min, increased to 110°C at a rate of 20°C/min, and held for 3 min, and finally raised to 280°C at a rate of 2°C/min and held for 3 min. The solvent delay time was set at 9 min and the total time of the program was up to 97 min. The electron impact energy was set at 70 eV. 1 μL of each sample was injected in splitless mode. High purity helium was used as the carrier gas, with a column flow rate of 1.0 mL/min in constant-flow mode. The temperatures of injector, ion source and transfer line were 280, 230 and 280°C, respectively. First, a full scan of the mixed standard of 1000 μg/L was performed to obtain the total ion chromatogram (TIC) to identify the retention time, quantitative and qualitative ion of each target (Appendix A Fig. S1). Then, the chromatogram was divided into several windows in the selected ion monitoring (SIM) mode. Data were collected and stored by the centroid method. The time for each mass scan, the time interval and the scan speed were 0.35 sec, 0.05 sec and 1343 Da/sec, respectively.

1.4. Quality control and assurance

The instrumental analysis was subjected to strict quality control procedures. Quantification of samples was performed using an internal standard method (2-FB and PCB209, 200 μg/L). None of the target compound was detected in the blanks, including ultrapure water blanks and LDPE blanks. In addition, samples spiked with known amounts of surrogate standard mixtures, i.e., Nap-d8, Ace-d10, Phe-d10, Chry-d12 and Pery-d12, were also measured to estimate the repeatability and accuracy of the analytical method. The recoveries of surrogates were 78% ± 15% (Nap-d8), 96% ± 12% (Ace-d10), 89% ± 18% (Phe-d10), 88% ± 15% (Chry-d12), 94% ± 11% (Pery-d12) (n = 5), respectively. All the concentrations of target compounds are reported without recovery correction.

1.5. Calculating the partition coefficients between LDPE and water (K_{LDPE}) for the target compounds

The sorption kinetics of free dissolved HOCs in passive sampling can be described by the following model (Huckins et al., 1993):

$$C_{LDPE} = C_W(k_u/k_e)\,(1-\exp(-k_e t)) \quad (1)$$

where C_{LDPE} (μg/kg) and C_W (μg/L) are concentrations of the target compounds in LDPE andwater phase during extraction

time t (day), respectively; k_u (L/day) and k_e (kg/day) are the sorption and desorption rates, respectively.

When the passive sampling is conducted for sufficient time (i.e., t tends to infinity), a dynamic equilibrium can be established between environmental matrix and sorption phase for the target compounds (Vrana et al., 2005). Then, Eq. (1) can be simplified to Eq. (2):

$$C_{LDPE} = C_W(k_u/k_e) = C_W K_{LDPE}(\text{when } t = \infty) \quad (2)$$

Here, K_{LDPE} (L/kg) is defined as the partition coefficient for HOCs between LDPE and water. This equation indicates that the ratio of C_{LDPE}/C_W is equal to K_{LDPE} when the sampling time t is long enough ($t = \infty$).

According to Fick's first law, the sorption kinetics were regressed with an exponential function (i.e., BoxLucas1) (Bao et al., 2011):

$$y = a\left(1–e^{-bt}\right) \quad (3)$$

where y (L/kg) can be regarded as the effective concentration of target compounds in the sorption phase, a (L/kg) and b (day^{-1}) are both fitting coefficients. Based on Eq. (2), y can be replaced by C_{LDPE}/C_W in this study. Meanwhile, when t tends to approach infinity in Eq. (3), y (C_{LDPE}/C_W) can be identified as K_{LDPE}. In other words, we can directly obtain K_{LDPE} value from the fitting coefficient a.

Moreover, the fitting error of K_{LDPE} can be represented as Eq. (4) (Bao et al., 2011):

$$\Delta \log K_{LDPE} = \frac{\Delta a}{a \ln 10} \quad (4)$$

Actually, the time of sorption cannot not be infinity in laboratory experiments nor in field application; then, the theoretical equilibrium time (t_e, day) can be defined as the time when the differences between K_{LDPE} and C_{LDPE}/C_W are less than 5%:

$$t_e = \frac{\ln 20}{b} \quad (5)$$

2. Results and discussion

2.1. Simultaneous determination of PAHs and SPAHs by GC–MS

A satisfactory separation of 16 PAHs and 13 PAHs could be achieved in TIC (Appendix A Fig. S1) and in the SIM mode (Appendix A Fig. S2), respectively. The retention time, qualitative & quantitative ions for each target in the SIM mode are shown in Table 1. In full-scan mode, the peaks of NaP and NaP-d8 in TIC could not be separated completely; while in the SIM mode, these two compounds were effectively identified through different ion channels. In addition, 2-NF and 9-NA could be also acquired with sufficient sensitivity by the SIM mode (Appendix A Fig. S2).

Therefore, a quantitative method was established for simultaneously determining the target PAHs and SPAHs. The mixed standard solution of each target compound was set at seven concentration points (i.e., 10, 20, 50, 100, 200, 500, 1000 μg/L). The same amounts of internal standards (200 μg/L for both 2-FB and PCB209) were added in different gradient standard solutions. The limits of detection were calculated based on the standard deviation of seven matrix samples spiked with target compounds at concentrations of three times the signal-to-noise ratio. The limits of detection for the selected target compounds were between 0.22 (1-MF) and 8.82 (Phe) ng/L. The R^2 linearity factor for the standard curves ranged from 0.996 to 0.999 (Table 1), showing that these targets were well detected.

2.2. Sorption kinetics of the targets on LDPE film

The sorption kinetics of HOCs on LDPE film involves a dynamic re-partitioning process of the target compounds between LDPE and water. According to the "like-dissolves-like" rule, long chains in LDPE would combine with the functional groups of the target compounds by van der Waals forces and hydrogen bonds (Endo et al., 2011). Thus, the target compounds in the aqueous phase can be constantly sorbed by LDPE until it reaches dynamic equilibrium, i.e., when the concentration ratio of the target compounds between the two phases no longer changes with time (Branislav and Gerrit, 2002; Mayer et al., 2003).

The sorption kinetics for the target PAHs and SPAHs are shown in Fig. 1. It can be seen that most targets showed a similar trend of sorption kinetics on LDPE: the ratio of C_{LDPE}/C_W increased linearly during the beginning time period; then, it rose gradually until reaching equilibrium between LDPE and water upon 80 d of extraction (Fig. 1). The enrichment capacities (indicated by the ratio of C_{LDPE}/C_W in equilibrium) for high-ring PAHs (i.e., higher K_{ow} values) were much larger than those for low-ring PAHs. For example, the ratio C_{LDPE}/C_W of IncdP (5 rings) in equilibrium was one order of magnitude greater than the value of Flua (3 rings) (Fig. 1a, and b). Due to their relatively small molecular weights, low-ring PAHs or SPAHs could easily enter or come out of the micro pores of LDPE film, and possibly need a longer time to reach equilibrium. In contrast, once high-ring targets were captured by the adsorbed phase, they could not be easily desorbed (Endo et al., 2019). This result was also consistent with the conclusion by Huckins et al. (1999), namely, the sorption phase of passive sampling showed a larger enrichment capacity for HOCs with higher K_{ow} values.

Notably, the data points of two SPAHs, i.e.,7-NBA and BA-7,12-D, showed great deviations from the sorption kinetics (Appendix A Fig. S2). They could not effectively fit within the exponential function (Eq. (3)), which may lead to large uncertainties in the fitted parameters. According to the previous report, these uncertainties might be induced by photochemical transformation during the pretreatment or analysis procedure (Qiao et al., 2013). Therefore, relevant indexes of these two compounds are not reported in this study.

2.3. The partition coefficient (K_{LDPE}) between LDPE and water for PAHs and SPAHs

All kinetic points for these targets (except for 7-NBA and BA-7,12-D) were treated equally in the determination of K_{LDPE}. Fitted parameters were obtained from a regression of the

Table 1 – The retention time, qualitative & quantitative ions, R^2 of linearity, and limit of detection for the target compounds.

No.	Target [a]	Types [b]	Channel	Retention (min)	Quantitative * & Qualitative ion	R^2	Limit of detection (ng/L)
1	NaP-d8	SS	–	9.676	136*,108,137	–	–
2	NaP	PAH	2	9.766	128*,102	0.9985	3.23
3	2-MN	SPAH	2	12.756	142*,141,115	0.9991	6.48
4	2-FB	IS	–	15.377	172*,171,170	–	–
5	2,6-DMN	SPAH	2	16.115	156*,141,155	0.9988	1.55
6	Acy	PAH	2	19.545	152*,76,126	0.9990	1.59
7	Ace-d10	SS	–	20.270	162*,164,160	–	–
8	Ace	PAH	2	20.533	154*,152,76	0.9985	2.25
9	Fluo	PAH	2	24.160	166*,165,167	0.9987	3.88
10	9-FL	SPAH	2	31.494	180*,152,126	0.9982	1.89
11	Phe-d10	SS	–	31.992	188*,94,80	–	–
12	Phe	PAH	3	32.183	178*,89,152	0.9978	8.82
13	Ant	PAH	3	32.443	178*,89,152	0.9966	1.23
14	3,6-DMP	SPAH	3	38.544	206*,191,178	0.9974	0.55
15	AQ	SPAH	3	40.471	208*,180,152	0.9990	2.43
16	Flua	PAH	3	41.822	202*,200,101	0.9993	0.41
17	Pyr	PAH	4	43.930	202*,200,101	0.9989	0.96
18	2-MAQ	SPAH	3	44.229	222*,165,194	0.9986	0.83
19	2-NF	SPAH	2	44.353	165*,211,164	0.9818	1.92
20	9-NA	SPAH	3	45.429	176*,223,165	0.9915	3.21
21	1-MF	SPAH	3	46.154	216*,200,189	0.9923	0.22
22	BaA	PAH	4	53.651	228*,113,200	0.9981	2.21
23	Chry-d12	SS	–	54.001	240*,236,241	–	–
24	Chry	PAH	4	54.226	228*,226,113	0.9985	2.23
25	3-NF	SPAH	3	57.346	217*,200,247	0.9914	1.83
26	BA-7,12-D	SPAH	4	58.522	258*,230,200	0.9985	0.94
27	1-NP	SPAH	4	59.235	201*,200,247	0.9880	1.59
28	PCB209	IS	–	60.918	498*,214,430	–	–
29	BbF	PAH	4	62.102	252*,253,250	0.9986	1.82
30	BkF	PAH	4	62.289	252*,253,250	0.9982	1.21
31	7-NBA	SPAH	4	63.755	215*,226,273	0.9983	1.44
32	BaP	PAH	5	65.473	252*,253,250	0.9960	0.35
33	Pery-d12	SS	–	66.458	264*,265,260	–	–
34	IncdP	PAH	5	79.281	276*,138,277	0.9973	0.54
35	DBA	PAH	5	79.719	278*,279,139	0.9975	0.35
36	BghiP	PAH	6	84.808	276*,137,138	0.9978	0.69

[a] The full names of these compounds are shown in Appendix A Table S1 and S2.
[b] SS indicates that the compound was used as a surrogate standard. NPAH, MPAH and OPAH indicate nitro-PAHs, methyl-PAHs, and oxy-PAHs. IS shows that the compound acted as an internal standard.
* Indicates the quantitative ion for the selected target.

measured data with Fick's first law of diffusion (i.e., Eq. (3)), and the details are shown in Table 2. The range was 0.90–0.99 for the least-square regression coefficients (R^2) and the p values for the fitting function were less than 0.05, respectively, indicating the good quality of the kinetic data fivalue.

The t_e of PAHs estimated with Eq. (5) ranged from 19 to 38 days (Table 2), which was consistent with the values in previous reports (Bao et al., 2012; Hawthorne et al., 2011). The t_e values of SPAHs were similar to those of PAHs. The t_e values exhibited a decreasing trend with increasing numbers of rings in PAHs or SPAHs (SI Fig. S4A). For example, the t_e value of NaP (2 ring) was 38.3 days, which was over two times longer than the t_e value of DBA (5 ring, t_e = 19.5 days). Notably, we can even conclude the presence of linear relationships between the average t_e values of PAHs or SPAHs and ring numbers (R^2 = 0.9529, p = .0158, Appendix A Fig. S4B). Some other reports also have found that passive sampling sorbents can easily concentrate nonpolar compounds within lipid-rich matrices (Bao et al., 2011; Durig et al., 2016), so the process of approaching equilibrium was more rapid for high-ring PAHs or SPAHs.

The sorption equilibrium time for different HOCs in passive sampling showed great variations, e.g., several hours to several months (Appendix A Table S3). Generally, the sorption process of HOCs on the sorbent in passive sampling may include three mass transfer steps: (1) external mass transfer, i.e., the diffusion of HOCs in the water films around the sorbent; (2) internal mass transfer, i.e., the diffusion of HOCs from the sorbent's surface to its interspace; and (3) adsorption of HOCs on active sties (Guo et al., 2019). Different equilibrium times of HOCs on the sorbent are significantly influenced by these three mass transfer limiting steps, which may be related to the characteristics of sorbent, properties of target compounds, and environmental factors. For example, polyethylene was proved to have a spongy and porous internal structure, which enabled the entrance and transport

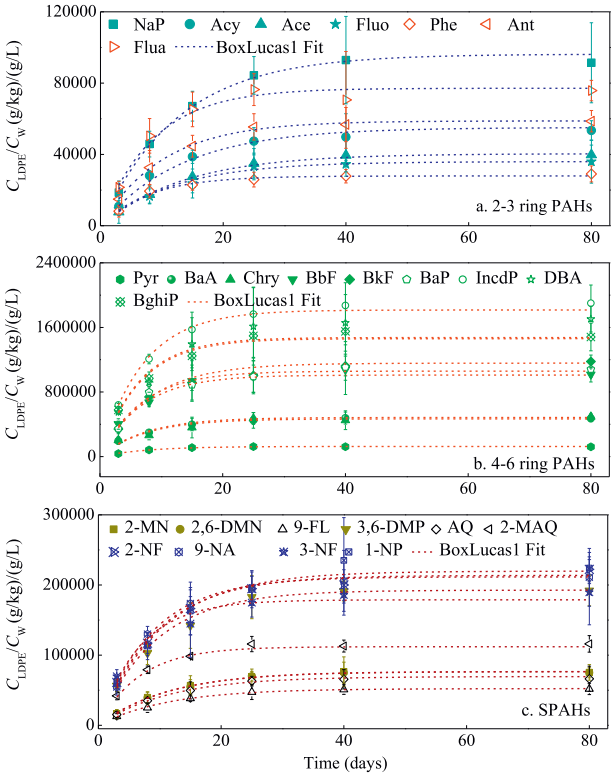

Fig. 1 – Sorption kinetics of the target PAHs (a and b) and SPAHs (c) on low density polyethylene (LDPE) expressed as C_{LDPE}/C_W versus time (days), where C_{LDPE} and C_W are the concentrations of the targets in LDPE film and water, respectively.

of organic chemicals (Wang and Wang, 2018). It was found that the moderately hydrophobic chemicals (e.g., $3 < \log K_{OW} < 5$) had relatively higher uptake rates (k_u) than hydrophilic chemicals ($\log K_{OW} < 3$), while the release rate (k_e) decreased with increasing $\log K_{OW}$, which indicated that the hydrophilic chemicals have higher elimination rates (Gao et al., 2019). Additionally, some environmental factors, such as temperature, pH, salinity and dissolved organic matter, could also affect the sorption behaviors of HOCs (Lei et al., 2018b; Lin et al., 2018b; Guo et al., 2019). Therefore, both laboratory tests and field deployment need to be carefully considered to give practicable results for monitoring HOCs by passive sampling.

The enrichment of a PAH in the sorption phase in passive sampling is associated with its K_{OW}; namely, the compounds with higher K_{OW} values often possess a greater enrichment capacity in equilibrium (Huckins et al., 2002), e.g., see Fig. 1a and b in this study. The K_{LDPE} values for PAHs or SPAHs also increased as their K_{ow} values increased (Table 2). In addition, except for two high-ring PAHs (i.e., DBA and BghiP), the K_{LDPE} values of the target PAHs in this study were in good agreement with the measured values that had been previously reported with similar treatment (Bao et al., 2012). The relative standard deviation between the two studies was less than 10% (Table 2), further verifying the reliability of the results in this study. The reported K_{LDPE} values of DBA and BghiP were 20% higher than their experimental values. This may be due to the different extraction methods for PAHs in the two studies, i.e., solid phase extraction in this study and liquid–liquid extraction used in Bao's study (Bao et al., 2012), respectively. However, regarding K_{LDPE} values of SPAHs, they have not been reported as far as we know. These might need further verification to obtain a better understanding of the bioavailability and toxicity of SPAHs in aquatic ecosystems.

A comparison of experimental log K_{LDPE} (i.e., the fitted log K_{LDPE}) and theoretical log K_{LDPE} (i.e., log $K_{LDPE} = 0.972 \times \log K_{OW} - 0.13$, (Booij et al., 2003)), indicated a certain correlation trend for high-ring PAHs and significant differences for low-ring PAHs or SPAHs, respectively (Table 2). There are several possible reasons for this result: The theoretical log K_{LDPE} values were calculated only from the K_{OW} values of the targets. This assumes that the enrichment capacity of LDPE for HOCs depends only on their K_{OW} values, but is independent of the molecular size or polarity of the targets. This is an ideal situation, which may differ from the actual measurement practice (Liu et al., 2018). For example, highly hydrophobic compounds have been demonstrated to be more difficult to desorb from the sorption phase in passive sampling (Huckins et al., 1993; Litten et al., 1993). In addition, the theoretical log K_{LDPE} values calculated by the formula were based on a statistical analysis that did not contain all 16 priority PAHs (Booij et al., 2003). Some inappropriate data were also deleted and the formula was optimized, which may lead to deviations between the theoretical values and the experimental values of log K_{LDPE}. For example, the fitting formula omits the samples with a higher relative standard deviation (more than 40%). Specific PAHs, whose molecular weights were less than Phe and greater than Chry, were also not excluded in the fitting formula (Lohmann, 2011).

Meanwhile, the theoretical log K_{LDPE} shown in Table 2, (i.e., log $K_{LDPE} = 0.972 \times \log K_{OW} - 0.13$), presented a linear relationship between log K_{LDPE} and log K_{OW} values (Booij et al., 2003). In this study, significant linear relationships were also observed for both PAHs (log $K_{LDPE} = 0.705 \times \log K_{OW} + 1.534$, $R^2 = 0.7113$, $p < 0.001$) and SPAHs (log $K_{LDPE} = 0.458 \times \log K_{OW} + 3.092$, $R^2 = 0.5609$, $p = 0.0077$) (Fig. 2). In previous studies, this kind of linear relationship has been applied to calculate K_{LDPE} values of some targets in practical application to reduce some of the work in passive sampling (Booij et al., 2003; Lohmann, 2011). However, when we combine the log K_{LDPE} values of PAHs and SPAHs together, it is difficult to fit these data by just a single linear formula.

In other studies, curvilinear relationships between measured log K_{LDPE} and log K_{OW} were observed for polybrominated diphenyl ethers (PBDEs) or polychlorinated biphenyls (PCBs) with similar treatments (Bao et al., 2011; Yang et al., 2006). The turning points of the log sorption-water partition coefficient (e.g., log K_{LDPE}) and log K_{OW} for those compounds were at log K_{OW} equal to 7–8. This kind of curvilinear relationship is similar to the correlations between log-based bioconcentration factors and log K_{OW} values for some HOCs observed in laboratory or field studies (Bao et al., 2011; Gerofke et al., 2005; Liu et al., 2017). This curvilinearity was thought to relate to the difference in the Gibbs free energies for cavity formation in the sorption phase (e.g., LDPE) and octanol, which might be more significant for larger molecules (e.g., $K_{ow} > 7$) (Yang et al., 2007b). Additionally, the target

Table 2 – Experimental and theoretical values of LDPE-water partition coefficient (K_{LDPE}) for the target PAHs and SPAHs, respectively.

Targets [α]	Types	$y = a(1\text{-}e^{-bx})$ [β]					Equilibrium time t_e (day)	Experimental log K_{LDPE} [γ]	Theoretical log K_{LDPE} [σ]	Reported log K_{LDPE} [ρ]
		a	Error of *a*	*b*	Error of *b*	R^2				
NaP	PAH	93,670	7594	0.0783	0.0147	0.9562	38.3	4.97 ± 0.035	3.15	NA [Ψ]
2-MN	SPAH	76,455	5173	0.0887	0.0132	0.9686	33.8	4.88 ± 0.029	3.16	NA
2,6-DMN	SPAH	74,276	2978	0.0927	0.0118	0.9793	32.3	4.87 ± 0.017	3.26	NA
Acy	PAH	53,794	2853	0.0856	0.0847	0.9849	35.0	4.73 ± 0.023	3.79	NA
Ace	PAH	37,728	2637	0.0841	0.0150	0.9471	35.6	4.58 ± 0.030	3.68	4.25 ± 0.12
Fluo	PAH	35,976	1815	0.0830	0.0093	0.9798	36.1	4.56 ± 0.022	3.93	4.51 ± 0.12
9-FL	SPAH	49,473	1347	0.0990	0.0071	0.9918	30.2	4.69 ± 0.012	3.58	NA
Phe	PAH	27,935	849	0.1250	0.0126	0.9779	24.0	4.45 ± 0.013	4.31	4.78 ± 0.12
Ant	PAH	57,985	1288	0.1036	0.0828	0.9846	28.9	4.76 ± 0.010	4.28	NA
3,6-DMP	SPAH	179,413	5253	0.1243	0.0099	0.9873	24.1	5.25 ± 0.013	3.74	NA
AQ	SPAH	67,633	2277	0.0931	0.0062	0.9921	32.2	4.83 ± 0.015	3.66	NA
Flua	PAH	77,128	1858	0.1164	0.0078	0.9927	25.7	4.89 ± 0.010	4.90	4.93 ± 0.14
Pyr	PAH	125,340	3348	0.1298	0.0113	0.9872	23.1	5.10 ± 0.012	4.94	5.07 ± 0.14
2-MAQ	SPAH	111,995	2487	0.1469	0.0104	0.9886	20.4	5.05 ± 0.010	3.99	NA
2-NF	SPAH	214,237	8022	0.0984	0.00948	0.9831	30.4	5.33 ± 0.016	4.49	NA
9-NA	SPAH	211,508	7126	0.1136	0.0085	0.9919	26.4	5.34 ± 0.015	4.20	NA
BaA	PAH	466,803	18,702	0.1331	0.0129	0.9533	22.5	5.67 ± 0.017	5.61	5.79 ± 0.15
Chry	PAH	484,163	25,267	0.1329	0.0251	0.9140	22.5	5.69 ± 0.023	5.61	5.70 ± 0.16
3-NF	SPAH	178,832	8836	0.1472	0.0163	0.9639	20.4	5.25 ± 0.021	5.26	NA
1-NP	SPAH	219,731	6047	0.0966	0.0069	0.9927	31.0	5.34 ± 0.012	4.49	NA
BbF	PAH	1,009,700	34,924	0.1465	0.0119	0.9743	20.4	6.00 ± 0.015	5.51	6.33 ± 0.13
BkF	PAH	1,121,780	43,293	0.1302	0.0143	0.9551	23.0	6.05 ± 0.017	5.70	6.56 ± 0.13
BaP	PAH	1,058,410	51,421	0.1469	0.0195	0.9596	20.4	6.02 ± 0.021	5.61	NA
IncdP	PAH	1,771,800	51,018	0.1482	0.0061	0.9949	20.2	6.25 ± 0.013	6.43	NA
DBA	PAH	1,460,420	172,248	0.1538	0.0256	0.9058	19.5	6.16 ± 0.051	6.19	7.20 ± 0.07
BghiP	PAH	1,474,350	67,907	0.1558	0.0143	0.9721	19.2	6.17 ± 0.020	6.21	7.36 ± 0.04

[α] The data points of 7-NBA and BA-7,12-D could not fit effectively within the exponential function (i.e., Eq. (3)) and may lead to large uncertainties for the fiand equilibrium parameters (SI Fig. S3). Thus, their relevant indexes are not reported in this study. Meanwhile, the value of 1-MF was also not obtained in this study due to some technical problems.

[β] In this equation, i.e., $y = a(1 - e^{-bt})$, y can be regarded as the effective concentration of target compounds in the sorption phase, *a* and *b* are both fitting coefficients. When *t* tends to approach infinity in Eq. (3), y (C_{LDPE}/C_W) can be identified as K_{LDPE}. Therefore, K_{LDPE} values could be directly obtained from the fitting coefficient *a*. The sorption kinetics were regressed with an exponential function in OriginPro 8.5 (Fitting/ Exponent Fit/ BoxLucas1).

[γ] Fitted parameters were obtained from a regression of measured data with Fick's first law of diffusion, i.e., $y = a(1 - e^{-bt})$ (Eq. (3)).

[σ] The theoretical formula, $\log K_{LDPE} = 0.972 \times \log K_{OW} - 0.13$, was adopted from (Booij et al., 2003). K_{OW} indicates the octanol–water partition coefficient, which were obtained from (Mackay et al., 1992; Qiao et al., 2014a).

[ρ] The reported values of log K_{LDPE} for PAHs were adopted from a previous publication with a similar method (Bao et al., 2012).

[Ψ] NA, not available.

compounds might not reach equilibrium with enough time under the interference of a third phase (e.g., LDPE) (Jonker and van der Heijden, 2007). They also concluded that the lack of hydrophobicity cutoff was only applicable to compounds with log K_{OW} up to 7.5. In this study, log K_{OW} values of PAHs and SPAHs were all less than 7, so no turning point or curvilinear relationship was observed (Fig. 2).

When conducting passive sampling in field applications, C_w is obtained from measured C_{LDPE} coupled with laboratory-calibrated log K_{LDPE} based on Eq. (2) as mentioned above. Actually, there is considerable doubt about whether C_{LDPE}/C_w can be regarded as K_{LDPE} since this value is usually calibrated within a fisinc time (Bao et al., 2011). In this study, the sorption kinetics showed that the extraction time of 38 days was sufficient enough to obtain the correlation between logK_{LDPE} and logK_{OW} (Fig. 1 and Table 2). Generally, it is suggested to maintain measurement for a longer time than the equilibrium time during passive sampling in field applications, e.g., a measurement time of more than 38 days for PAHs or SPAHs, can guarantee the accuracy of the experimental results. In order to precisely determine the concentration of target compounds by LDPE, it has been recommended to acquire the K_{LDPE} values as close to the actual field conditions (e.g., pH, temperature, salinity and DOM) as possible (Lei et al., 2018b; Liu et al., 2018; Liu et al., 2013).

Furthermore, LDPE with the same thickness (i.e., 50 μm), purchased from Runfang Co. Ltd., Zhenjiang, China, was subjected to the same pretreatments to determine K_{LDPE} for comparison purposes. According to the Eq. (2), i.e., $C_{LDPE} = C_W(k_u/k_e) = C_W K_{LDPE}$ (when $t = \infty$), the result indicates that the ratio of C_{LDPE}/C_W is equal to K_{LDPE} when the sampling time *t* is long enough ($t = \infty$). In this study, however, 38 days was proven to be sufficient for PAHs or SPAHs to reach equilibrium for LDPE purchased from TRM manufacturing, so we considered that 60 days was sufficient for the LDPE purchased from

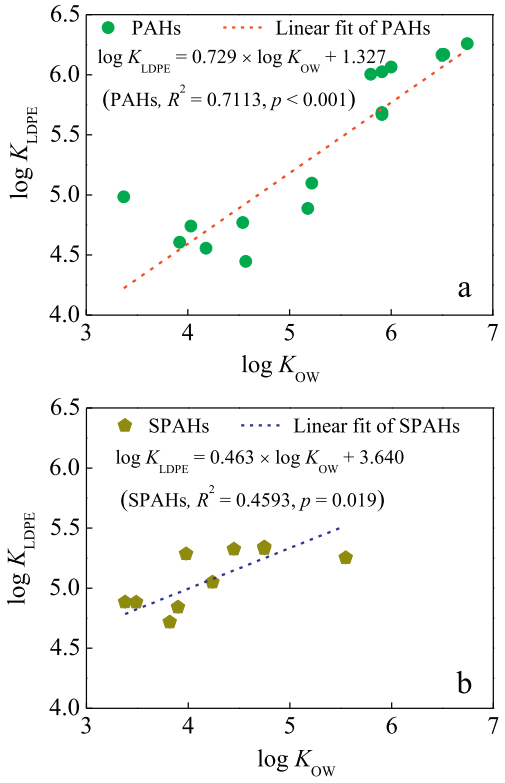

Fig. 2 – The relationships of log K_{LDPE} and log K_{OW} for the PAHs (a) and SPAHs (b).

Runfang Co. Ltd. For simplicity, these K_{LDPE} values were calculated by using log (C_{LDPE}/C_w) at 60 days. The results showed that log K_{LDPE} values of most PAHs and SPAHs determined by the LDPE from TRM were significantly higher than those of LDPE from Runfang ($p < 0.05$) (Fig. 3). Taking NaP as an example, the K_{LDPE} values for the two materials were 3.39 (Runfang) and 4.97 (TRM), respectively, which indicated that the LDPE produced by TRM had higher enrichment capacity for NaP. Therefore, a lower mass of LDPE would be needed when designing a passive sampler. This also allowed our passive sampler to be smaller in field applications, with higher resolution and detection limits for the targets. Additionally, there was no significant difference for the log K_{LDPE} of 2-MAQ, BaA, 3-NP and 1-NP between materials from the two companies. The properties of LDPE from the two companies such as aperture, composition, and degree of crystallinity may contribute to the differences (Guo et al., 2019), and the material properties should be further explored in future studies.

2.4. The verification of the "zero sink" assumption for the target PAHs and SPAHs in LDPE

To achieve a successful time-weighted average (TWA) concentration in passive sampling, "zero sink" is one of the most important prerequisites that must be satisfied (Chen and Pawliszyn, 2003; Liu et al., 2013). This theory considers that the targets diffusing to the surface of the sorbent phase (e.g., LDPE) are immediately dragged into its interior so that their concentration at the surface can be regarded as zero (Liu et al., 2013; Ouyang et al., 2005). This ensures that the rate of mass loading of additional target is not affected when it is sorbed by the sorbent phase (Chen and Pawliszyn, 2003).

In the present study, the zero-sink effect for LDPE was tested by an empirical approach based on intermittent and continuous exposure to a solution spiked with the target compounds. The procedure of this experiment was similar to that in a previous report (Liu et al., 2013). In brief, 1 L ultrapure water, spiked with target compounds at an initial concentration of 0.02 and 0.05 μg/L, respectively, was added into glass media bottles. Sodium azide (NaN_3) was also added into each bottle at 200 mg/L to inhibit microbial activity. The mixture was stirred at 100 r/min for 2 hr to evenly mix the solution. Six identical LDPE strips were exposed to the preset solution for 6 days under static conditions. Three LDPE strips were taken out, rinsed, and extracted with solvent as mentioned

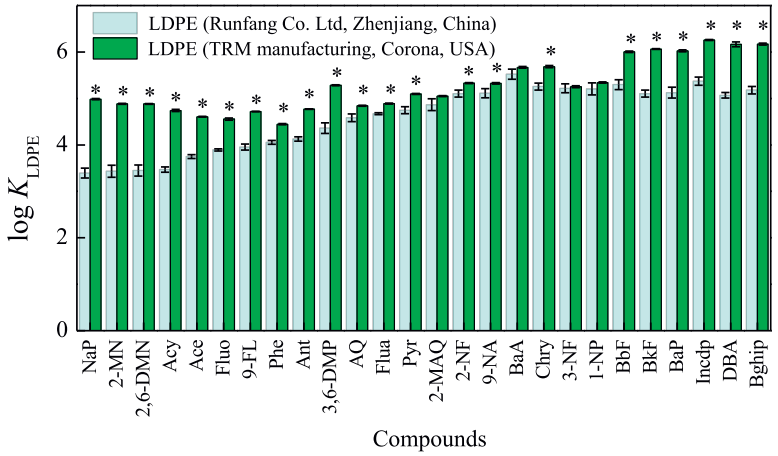

Fig. 3 – Values of the LDPE-water partition coefficient (K_{LDPE}) for target PAHs and SPAHs. LDPE membranes were purchased from two companies, Runfang Co. Ltd., Zhenjiang, China and TRM manufacturing, Corona, USA. The asterisk above the bars indicates a significant difference between log K_{LDPE} values from the two companies (one-way ANOVA, *, $p < 0.05$; without *, $p > 0.05$).

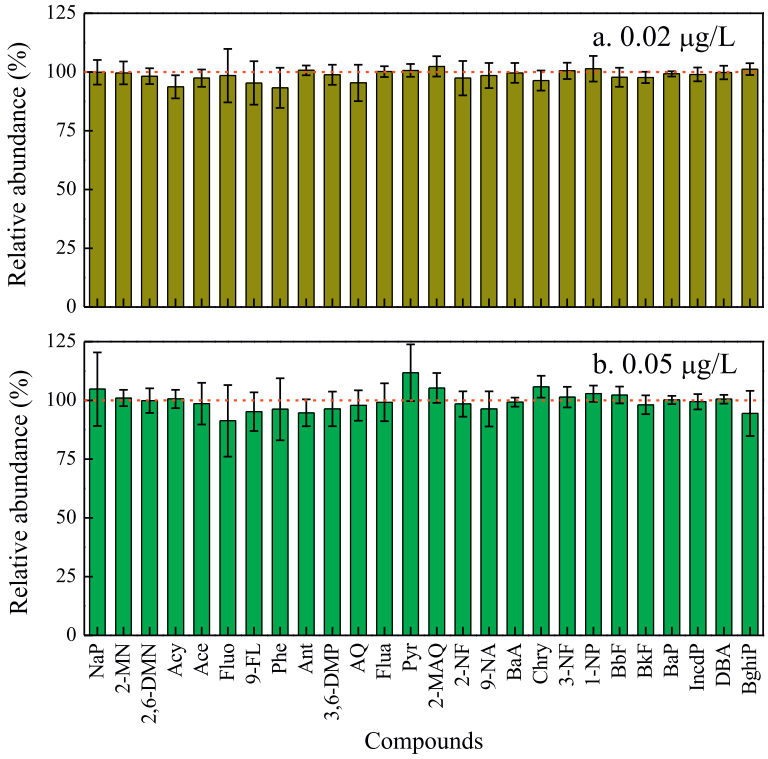

Fig. 4 – Verification of "zero sink" for target PAHs and SPAHs in LDPE. Relative abundances of the target masses in LDPE strips were obtained through sorption and desorption stages. The initial concentration of each target compound was set as 0.02 μg/L (a) and 0.05 μg/L (b), respectively.

above, to determine the initial amounts of targets loaded in the sorption stage. Subsequently, the other remaining LDPE strips were taken out, rinsed, and immersed in purified water again without spiking with target compounds, to conduct the desorption stage for 6 days as well.

When the target masses in LDPE from the sorption and desorption stages were approximately equal to each other (i.e., relative abundances equal to 100%), the "zero sink" hypothesis would be perfectly verified (Liu et al., 2013). The relative abundances acquired in this study ranged from 93.3% ± 4.93% to 102% ± 4.35% and 91.3% ± 15.3% to 112% ± 12.1% at an initial concentration of 0.02 and 0.05 μg/L, respectively (Fig. 4), showing that negligible losses of each target compound occurred from the loaded LDPE during the desorption exposure. These results indicated that the concentration of targets at the interface between LDPE and water could be regarded as zero. In other words, LDPE has been verified to act as a "zero sink" for the target PAHs and SPAHs in passive sampling.

3. Conclusions

Low-density polyethylene (LDPE) has been widely used for passive sampling of HOCs in aquatic environments. For determination of freely dissolved concentrations of HOCs, measurement of the LDPE-water partition coefficients (K_{LDPE}) in the laboratory is a critical step before field application. In this study, 16 priority PAHs and some typical SPAHs were simultaneously determined by GC–MS to explore their adsorption kinetics on LDPE film. The results showed that the equilibrium times for the target PAHs and SPAHs ranged from 19 to 38 days. The experimental K_{LDPE} values of 16 priority PAHs were in good agreement with previously reported values, and the K_{LDPE} values of the target SPAHs were reported for the first time in this study. Significant linear relationships were observed for both PAHs and SPAHs. Most of the determined log K_{LDPE} were higher than the corresponding theoretical values calculated by the empirical formula, which was based on their K_{OW} values. Moreover, the selected LDPE film was also proven to meet the condition of "zero sink" for the target compounds. These results provide strong support for the design and field application of passive samplers, which could be a powerful tool for assessment of ecological risk, bioavailability and in situ remediation efficiency.

Acknowledgements

This study was supported by the National Natural Science Foundation of China (Nos. 41877471 and 41676095), the China Postdoctoral Science Foundation, China (No. 2017M622782) and the Open Foundation of Key Laboratory of Tropical Marine Bio-resources and Ecology (LMB), Chinese Academy of Sciences, China (No. LMB20191004) and the Science and Technology Innovation Commission of Shenzhen, China (No.

JCYJ20180507182227257). In-kind support of low-density polyethylene (LDPE) film purchase was provided by Dr. Ji Luo in the University of California, Riverside. Technical guidance on GC–MS analysis was supported by Zhuo Man (Senior Engineer) in PerkinElmer Instruments (Shanghai) Co., Ltd., and Dr. Meng Qiao (Assistant Professor) in the Research Center for Eco-Environmental Sciences, Chinese Academy of Sciences. We also thank the anonymous reviewers for their constructive comments and suggestions.

Appendix A. Supplementary data

Supplementary data to this article can be found online at https://doi.org/10.1016/j.jes.2019.07.021.

REFERENCES

Ahrens, L., Daneshvar, A., Lau, A.E., Kreuger, J., 2018. Concentrations, fluxes and field calibration of passive water samplers for pesticides and hazard-based risk assessment. Sci. Total Environ. 637, 835–843.

Arp, H.P.H., Hale, S.E., Marie, E.K., Gerard, C., Grabanski, C.B., Miller, D.J., et al., 2015. Review of polyoxymethylene passive sampling methods for quantifying freely dissolved porewater concentrations of hydrophobic organic contaminants. Environ. Toxicol. Chem. 34, 710–720.

Bao, L.J., You, J., Zeng, E.Y., 2011. Sorption of PBDE in low-density polyethylene film: implications for bioavailability of BDE-209. Environ. Toxicol. Chem. 30, 1731–1738.

Bao, L.J., Xu, S.P., Liang, Y., Zeng, E.Y., 2012. Development of a low-density polyethylene-containing passive sampler for measuring dissolved hydrophobic organic compounds in open waters. Environ. Toxicol. Chem. 31, 1012–1018.

Booij, K., Sleiderink, H.M., Smedes, F., 1998. Calibrating the uptake kinetics of semipermeable membrane devices using exposure standards. Environ. Toxicol. Chem. 17, 1236–1245.

Booij, K., Hoedemaker, J.R., Bakker, J.F., 2003. Dissolved PCBs, PAHs, and HCB in pore waters and overlying waters of contaminated harbor sediments. Environ. Sci. Technol. 37, 4213–4220.

Booij, K., Robinson, C.D., Burgess, R.M., Mayer, P., Roberts, C.A., Ahrens, L., et al., 2016. Passive sampling in regulatory chemical monitoring of nonpolar organic compounds in the aquatic environment. Environ. Sci. Technol. 50, 3–17.

Borrelli, R., Tcaciuc, A.P., Verginelli, I., Baciocchi, R., Guzzella, L., Cesti, P., Zaninetta, L., et al., 2018. Performance of passive sampling with low-density polyethylene membranes for the estimation of freely dissolved DDx concentrations in lake environments. Chemosphere 200, 227–236.

Branislav, V., Gerrit, S., 2002. Calibrating the uptake kinetics of semipermeable membrane devices in water: impact of hydrodynamics. Environ. Sci. Technol. 36, 290–296.

Chen, Y., Pawliszyn, J., 2003. Time-weighted average passive sampling with a solid-phase microextraction device. Anal. Chem. 75, 2004–2010.

Chen, H., Chen, S., Quan, X., Zhao, Y.Z., Zhao, H.M., 2008. Solubility and sorption of petroleum hydrocarbons in water and cosolvent systems. J. Environ. Sci. (China) 20, 1177–1182.

Cornelissen, G., Wiberg, K., Broman, D., Arp, H.P.H., Persson, Y., Sundqvist, K., Jonsson, P., 2008. Freely dissolved concentrations and sediment-water activity ratios of PCDD/fs and PCBs in the open Baltic Sea. Environ. Sci. Technol. 42, 8733–8739.

Durig, W., Blakey, I., Grant, S., Chambers, L., Escher, B.I., Weijs, L., Gaus, C., 2016. New polymer passive sampler for sensitive biomonitoring of lipid-rich matrices. Environ. Sci. Technol. Lett. 3, 52–56.

Endo, S., Hale, S.E., Goss, K.U., Arp, H.P.H., 2011. Equilibrium partition coefficients of diverse polar and nonpolar organic compounds to Polyoxymethylene (POM) passive sampling devices. Environ. Sci. Technol. 45, 10124–10132.

Endo, S., Matsuura, Y., Vermeirssen, E.L.M., 2019. Mechanistic model describing the uptake of chemicals by aquatic integrative samplers: comparison to data and implications for improved sampler configurations. Environ. Sci. Technol. 53, 1482–1489.

Forsberg, N.D., Wilson, G.R., Anderson, K.A., 2011. Determination of parent and substituted polycyclic aromatic hydrocarbons in high-fat salmon using a modified QuEChERS extraction, dispersive SPE and GC-MS. J. Agr. Food Chem. 59, 8108–8116.

Gao, X.Z., Xu, Y.P., Ma, M., Rao, K.F., Wang, Z.J., 2019. Simultaneous passive sampling of hydrophilic and hydrophobic emerging organic contaminants in water. Ecotox. Environ. Safe. 178, 25–32.

Gerofke, A., Kömp, P., McLachlan, M.S., 2005. Bioconcentration of persistent organic pollutants in four species of marine phytoplankton. Environ. Toxicol. Chem. 24, 2908–2917.

Gilbert, D., Mayer, P., Pedersen, M., Vinggaard, A.M., 2015. Endocrine activity of persistent organic pollutants accumulated in human silicone implants - dosing in vitro assays by partitioning from silicone. Environ. Int. 84, 107–114.

Gómez, M.J., Herrera, S., Solé, D., Garcíacalvo, E., Fernándezalba, A. R., 2012. Spatio-temporal evaluation of organic contaminants and their transformation products along a river basin affected by urban, agricultural and industrial pollution. Sci. Total Environ. 420, 134–145.

Guo, X., Chen, C., Wang, J.L., 2019. Sorption of sulfamethoxazole onto six types of microplastics. Chemosphere 228, 300–308.

Hawthorne, S.B., Jonker, M.T., Grabanski, C.B., Azzolina, N.A., Miller, D.J., 2011. Measuring picogram per liter concentrations of freely dissolved parent and alkyl PAHs (PAH-34), using passive sampling with polyoxymethylene. Anal. Chem. 83, 6754–6761.

Huckins, J.N., Manuweera, G.K., Petty, J.D., Mackay, D., Lebo, J.A., 1993. Lipid-containing semipermeable membrane devices for monitoring organic contaminants in water. Environ. Sci. Technol. 27, 2489–2496.

Huckins, J.N., Petty, J.D., Orazio, C.E., 1999. Determination of uptake kinetics (sampling rates) by lipid-containing semipermeable membrane devices (SPMDs) for polycyclic aromatic hydrocarbons (PAHs) in water. Environ. Sci. Technol. 33, 3918–3923.

Huckins, J.N., Petty, J.D., Prest, H.F., Clark, R., Alvarez, D., Orazio, C., et al., 2002. A guide for the use of semipermeable membrane devices (SPMDs) as samplers of waterborne hydrophobic organic contaminants. API Publ. 4690, 1–192.

Jonker, M.T., van der Heijden, S.A., 2007. Bioconcentration factor hydrophobicity cutoff: an artificial phenomenon reconstructed. Environ. Sci. Technol. 41, 7363–7369.

Joyce, A.S., Portis, L.M., Parks, A.N., Burgess, R.M., 2016. Evaluating the relationship between equilibrium passive sampler uptake and aquatic organism bioaccumulation. Environ. Sci. Technol. 50, 11437–11451.

Knecht, A.L., Goodale, B.C., Truong, L., Simonich, M.T., Swanson, A.J., Matzke, M.M., et al., 2011. Comparative developmental toxicity of environmentally relevant oxygenated PAHs. Toxicol. Appl. Pharm. 271, 266–275.

Kojima, Y., Inazu, K., Hisamatsu, Y., Okochi, H., Baba, T., Nagoya, T., 2010. Influence of secondary formation on atmospheric occurrences of oxygenated polycyclic aromatic hydrocarbons in airborne particles. Atmos. Environ. 44, 2873–2880.

Lao, W.J., Maruya, K.A., Tsukada, D., 2019. An exponential model based new approach for correcting aqueous concentrations of hydrophobic organic chemicals measured by polyethylene passive samplers. Sci. Total Environ. 646, 11–18.
Lei, P., Zhang, H., Shan, B., Zhang, B., 2016. Distribution, diffusive fluxes, and toxicity of heavy metals and PAHs in pore water profiles from the northern bays of Taihu Lake. Environ. Sci. Pollut. Res. 23 (21), 1–12.
Lei, P., Pan, K., Zhang, H., Bi, J., 2018a. Pollution and risk of PAHs in surface sediments from the tributaries and their relation to anthropogenic activities, in the main urban districts of Chongqing City, Southwest China. B. Environ. Contam. Tox. 103, 28–33.
Lei, P., Shan, B., Zhang, H., 2018b. Development and application for passive sampling techniques in water environment, a review. Environ. Chem. 37, 480–496 (in Chinese).
Li, Y.Y., Wang, H.T., Xia, X.H., Zhai, Y.W., Lin, H., Wen, W., et al., 2018. Dissolved organic matter affects both bioconcentration kinetics and steady-state concentrations of polycyclic aromatic hydrocarbons in zebrafish (*Danio rerio*). Sci. Total Environ. 639, 648–656.
Lin, W., Jiang, R.F., Shen, Y., Xiong, Y.X., Hu, S.Z., Xu, J.Q., et al., 2018a. Effect of dissolved organic matter on pre-equilibrium passive sampling: a predictive QSAR modeling study. Sci. Total Environ. 635, 53–59.
Lin, H., Xia, X.H., Bi, S.Q., Jiang, X.M., Wang, H.T., Zhai, Y.W., et al., 2018b. Quantifying bioavailability of pyrene associated with dissolved organic matter of various molecular weights to *Daphnia magna*. Environ. Sci. Technol. 52, 644–653.
Litten, S., Mead, B., Hassett, J., 1993. Application of passive samplers (pisces) to locating a source of PCBs on the Black River, New York. Environ. Toxicol. Chem. 12, 639–647.
Liu, H.H., Bao, L.J., Zhang, K., Xu, S.P., Wu, F.C., Zeng, E.Y., 2013. Novel passive sampling device for measuring sediment-water diffusion fluxes of hydrophobic organic chemicals. Environ. Sci. Technol. 47, 9866–9873.
Liu, H.H., Wei, M.B., Yang, X.H., Yin, C., He, X., 2017. Development of TLSER model and QSAR model for predicting partition coefficients of hydrophobic organic chemicals between low density polyethylene film and water. Sci. Total Environ. 574, 1371–1378.
Liu, C., Zhang, W., Shan, B., 2018. Passive enrichment of endocrine disrupting chemicals(EDCs) by low-density polyethylene (LDPE)membrane from solutions. Acta Sci. Circum. 38, 2641–2649 (in Chinese).
Lohmann, R., 2011. Critical review of low-density polyethylene's partitioning and diffusion coefficients for trace organic contaminants and implications for its use as a passive sampler. Environ. Sci. Technol. 46, 606–618.
Lohmann, R., Muir, D., Zeng, E.Y., Bao, L.J., Allan, I.J., Arinaitwe, K., et al., 2017. Aquatic global passive sampling (AQUA-GAPS) revisited: frst steps toward a network of networks for monitoring organic contaminants in the aquatic environment. Environ. Sci. Technol. 51, 1060–1067.
Lydy, M.J., Landrum, P.F., Oen, A.M.P., Allinson, M., Smedes, F., Harwood, A.D., et al., 2014. Passive sampling methods for contaminated sediments: state of the science for organic contaminants. Integr. Environ. Asses. 10, 167–178.
Mackay, D., Shiu, W.Y., Ma, K.C., 1992. Illustrated handbook of physical-chemical properties and environmental fate for organic chemicals. Volume II: Polynuclear Aromatic Hydrocarbons, Polychlorinated Dioxins, and Dibenzofurans.
Manolis, T., Stephanou, E.G., 2007. Diurnal cycle of PAHs, nitro-PAHs, and oxy-PAHs in a high oxidation capacity marine background atmosphere. Environ. Sci. Technol. 41, 8011–8017.
Mayer, P., Tolls, J., Hermens, J.L., Mackay, D., 2003. Equilibrium sampling devices. Environ. Sci. Technol. 37, 184A–191A.
Mayer, P., Parkerton, T.F., Adams, R.G., Cargill, J.G., Gan, J., Gouin, T., et al., 2014. Passive sampling methods for contaminated sediments: scientific rationale supporting use of freely dissolved concentrations. Integr. Environ. Asses. 10, 197–209.
Meng, Y., Liu, X.H., Lu, S.Y., Zhang, T.T., Jin, B.C., Wang, Q., et al., 2019. A review on occurrence and risk of polycyclic aromatic hydrocarbons (PAHs) in lakes of China. Sci. Total Environ. 651, 2497–2506.
Moeckel, C., Monteith, D.T., Llewellyn, N.R., Henrys, P.A., Pereira, M.G., 2014. Relationship between the concentrations of dissolved organic matter and polycyclic aromatic hydrocarbons in a typical UK upland stream. Environ. Sci. Technol. 48, 130–138.
Mutzner, L., Vermeirssen, E.L.M., Ort, C., 2019. Passive samplers in sewers and rivers with highly fluctuating micropollutant concentrations - better than we thought. J. Hazard. Mater. 361, 312–320.
Ouyang, G., Chen, Y., Pawliszyn, J., 2005. Time-weighted average water sampling with a solid-phase microextraction device. Anal. Chem. 77, 7319–7325.
Qiao, M., Qi, W., Liu, H., Qu, J., 2013. Simultaneous determination of typical substituted and parent polycyclic aromatic hydrocarbons in water and solid matrix by gas chromatography–mass spectrometry. J. Chromatogr. A 1291, 129–136.
Qiao, M., Qi, W., Liu, H., Qu, J., 2014a. Occurrence, behavior and removal of typical substituted and parent polycyclic aromatic hydrocarbons in a biological wastewater treatment plant. Water Res. 52, 11–19.
Qiao, M., Qi, W., Liu, H., Qu, J., 2014b. Oxygenated, nitrated, methyl and parent polycyclic aromatic hydrocarbons in rivers of Haihe River system, China: occurrence, possible formation, and source and fate in a water-shortage area. Sci. Total Environ. 481, 178–185.
Qiao, M., Qi, W., Liu, H., Bai, Y., Qu, J., 2016. Formation of oxygenated polycyclic aromatic hydrocarbons from polycyclic aromatic hydrocarbons during aerobic activated sludge treatment and their removal process. Chem. Eng. J. 302, 50–57.
Sacks, V.P., Rainer, L., 2011. Development and use of polyethylene passive samplers to detect triclosans and alkylphenols in an urban estuary. Environ. Sci. Technol. 45, 2270–2277.
Tcaciuc, A.P., Apell, J.N., Gschwend, P.M., 2015. Modeling the transport of organic chemicals between polyethylene passive samplers and water in finite and infinite bath conditions. Environ. Toxicol. Chem. 34, 2739–2749.
Thuy, H.T.T., Loan, T.T.C., Phuong, T.H., 2018. The potential accumulation of polycyclic aromatic hydrocarbons in phytoplankton and bivalves in can Gio coastal wetland, Vietnam. Environ. Sci. Pollut. R. 25, 17240–17249.
Valderrama, J.F.N., Baek, K., Molina, F.J., Allan, I.J., 2016. Implications of observed PBDE diffusion coefficients in low density polyethylene and silicone rubber. Environ. Sci. Process Impacts 18, 87–94.
Vrana, B., Allan, I.J., Greenwood, R., Mills, G.A., Dominiak, E., Svensson, K., et al., 2005. Passive sampling techniques for monitoring pollutants in water. Trends Anal. Chem. 24, 845–868.
Wang, W.F., Wang, J., 2018. Comparative evaluation of sorpyion kinetics and isotherm of pyrene onto microplastics. Chemosphere 193, 567–573.
Wang, W., Jariyasopit, N., Schrlau, J., Jia, Y., Tao, S., Yu, T.W., et al., 2011. Concentration and photochemistry of PAHs, NPAHs, and OPAHs and toxicity of PM2.5 during the Beijing Olympic games. Environ. Sci. Technol. 45, 6887–6895.
Yang, Z.Y., Zeng, E.Y., Xia, H., Wang, J.Z., Mai, B.X., Maruya, K.A., 2006. Application of a static solid-phase microextraction procedure combined with liquid–liquid extraction to determine poly(dimethyl)siloxane-water partition coefficients for selected polychlorinated biphenyls. J. Chromatogr. A 1116, 240–247.
Yang, Z.Y., Greenstein, D., Zeng, E.Y., Maruya, K.A., 2007a. Determination of poly (dimethyl) siloxane – water partition

coefficients for selected hydrophobic organic chemicals using 14C-labeled analogs. J. Chromatogr. A 1148, 23–30.
Yang, Z.Y., Zhao, Y.Y., Tao, F.M., Ran, Y., Mai, B.X., Zeng, E.Y., 2007b. Physical origin for the nonlinear sorption of very hydrophobic organic chemicals in a membrane-like polymer film. Chemosphere 69, 1518–1524.
Zhu, T.Y., Wu, J., He, C.D., Pu, D.F., Wu, J., 2018. Development and evaluation of MTLSER and QSAR models for predicting polyethylene-water partition coefficients. J. Environ. Manag. 223, 600–606.